GROUND-BASED OBSERVATIONS OF THE VLF AURORAL HISS AT LOVOZERO AND BARENTSBURG OBSERVATORIES

A.S. Nikitenko (iD)
Polar Geophysical Institute RAS,
Apatity, Russia, alex.nikitenko91@gmail.com

N.G. Kleimenova (iD)
Schmidt Institute of Physics of the Earth of the RAS,
Moscow, Russia, ngk1935@yandex.ru

Yu.V. Fedorenko (iD)
Polar Geophysical Institute RAS,
Apatity, Russia, yury.fedorenko@gmail.com

E.B. Beketova (iD)
Apatity Branch of Murmansk Arctic University,
Apatity, Russia, elena.beketova@gmail.com

Abstract. The paper presents the results of the analysis of auroral hiss bursts, measured at Lovozero and Barentsburg observatories. These points are located on close geomagnetic meridians in the auroral and circumpolar zones. The auroral hiss bursts occur first in the auroral zone at Lovozero Observatory. Then, they fade out smoothly and occur in the circumpolar zone at Barentsburg Observatory. These events are observed when geomagnetic activity and the source of phase scintillation of GPS signals move from auroral to circumpolar latitudes. Analysis of magnetic field polarization and arrival angles of the bursts has shown that the area on the Earth surface, illuminated by hiss bursts, arose at auroral latitudes near Lovozero Observatory, and then moved to higher latitudes. Since propagation of the hiss to the ground and occurrence of GPS signal scintillation requires the presence of electron density irregularities of similar scales in the ionosphere, we assume that the same irregularities could cause both phenomena. A possible cause of their occurrence is the development of current-convective and (or) drift instability in the ionosphere caused by the development of field-aligned currents. Their development is indicated by the simultaneous recording of Pi1B pulsations. The results show that the termination of hiss at auroral latitudes may be caused by a shift of the geomagnetic disturbance region to high latitudes, rather than changes of wave propagation conditions in the ionosphere.

Keywords: GPS scintillation, auroral hiss, Pi1B pulsations.

INTRODUCTION

Auroral hiss is noise-like electromagnetic emission in the frequency range from several kilohertz to ~500 kHz with maximum intensity at frequencies 8–10 kHz [Makita, 1979; Sazhin et al., 1993]. This is one of the most common natural whistler emissions recorded both by satellites and on the Earth surface at high latitudes.

Hiss is generated as a result of the development of Cherenkov's instability of precipitating electrons with energies below 10 keV [Jørgensen, 1968; Maggs, 1976; Makita, 1979]. Numerous satellite observations have shown that these emissions correlate well with <1 keV electron fluxes [Hoffman, Laaspere, 1972; Mosier, Gurnett, 1972; Laaspere, Hoffman, 1976, etc.]. On the Earth surface, hiss is observed as bursts lasting from 1 to 10–20 min, which are often followed by an increase in the brightness of the auroras or their motion [Harang, Larsen, 1965; Makita, 1979; Nikitenko et al., 2022].

The condition for Cherenkov's resonance for the lower hiss range below ~30 kHz is observed for waves with wave normals lying at large angles to the external magnetic field [Sonwalkar, Harikumar, 2000]. Such waves cannot reach the Earth surface due to reflection at altitudes where their frequency coincides with the local lower hybrid frequency or reflection in the lower ionosphere, where there is a sharp refractive index gradient.

The generally recognized mechanism of auroral hiss propagation to the ground is scattering by small-scale (less than 1 km) irregularities in the upper ionosphere [Sonwalkar, Harikumar, 2000]. Scattered waves have a wide spatial spectrum. A portion of this spectrum falls into the so-called propagation cone and hence is able to reach the Earth surface. The concept of the propagation cone arises when considering ionospheric plasma as a medium whose parameters vary only with altitude. When propagating in such a medium, the horizontal component of the wave vector is conserved according to Snell's law. Boundaries of the cone are defined by waves in which the vertical component of the wave normal is zero near the Earth surface.

Auroral hiss is recorded near the Earth surface much less frequently than by satellites [Gurnett, 1966; Makita, 1979]. This fact indicates that ground-based observations of these emissions require ionospheric conditions that allow the waves to reach the Earth surface. The factors affecting the conditions of hiss propagation to Earth play an important role in studying the dynamics of ionospheric plasma.

Recent studies of auroral hiss in auroral latitudes have shown that these emissions are typical of the growth phase of a magnetospheric substorm and they suddenly stop with the onset of the substorm [Kleimenova et al., 2019]. The

authors have suggested that end of the bursts is due to increasing wave absorption in the ionosphere, which could be caused by energetic particle precipitation during breakup. Moreover, there was a close relationship between the occurrence of surface hiss bursts and amplification of field-aligned currents.

Manninen et al. [2020] have shown that in 58 of 65 events, when hiss was recorded at the Kannuslehto auroral station (Northern Finland), there was a region of field-aligned current amplification near this station. From VLF observations at the circumpolar station South Pole [Spasojevic, 2016], it has been found that hiss bursts are more likely to occur when the maximum intensity of field-aligned currents approaches the observation point in latitude.

As a rule, all the cited works have used the results of VLF observations only from one station at auroral or circumpolar latitudes. To date, no studies have been carried out on the latitudinal dynamics of the occurrence of auroral hiss on the Earth surface and comparisons between simultaneous observations at auroral and circumpolar latitudes.

In this paper, we for the first time examine the latitudinal dynamics of propagation of auroral hiss bursts to the Earth surface from simultaneous observations at two points located at different latitudes in the same longitude sector. We use data from Lovozero Auroral Observatory (LOZ, Kola Peninsula, geographical coordinates φ=67.97° N, λ=35.02° E, corrected geomagnetic coordinates (CGM) F=64.7°, Λ=113.1°) and Barentsburg Circumpolar Observatory (BAB, the Svalbard archipelago, φ=78.09 N, λ=14.21° E; F=75.21°, Λ=126.06°, CGM). Since auroral hiss bursts on the Earth surface are recorded mainly in winter [Manninen et al., 2020], we have selected VLF observations made in the winter of 2018–2019 for analysis. We have identified 17 events when the auroral hiss was detected at these points at adjacent time intervals, i.e. at almost the same hour. In eleven events, there were no clear coincidences in the occurrence of hiss bursts. In these events, hiss bursts at auroral latitudes (at LOZ) were generally observed during the growth phase of the substorm occurring on this meridian at auroral latitudes and were not recorded at BAB. Nonetheless, hiss bursts at BAB were accompanied by weak polar geomagnetic disturbances unrelated to substorms and appeared regardless of bursts at LOZ.

In 6 of 17 events, there was a clear sequence of hiss bursts: the bursts were recorded first at auroral (LOZ) and 10–15 min later at circumpolar (BAB) latitudes. Below are the results of the analysis of three of six most dramatic events: January 5, 2019, 21:00–22:00 UT; December 9, 2018, 19:00–20:00 UT; March 1, 2019, 18:00–20:00 UT.

1.   MATERIAL AND METHODS

The electromagnetic field of auroral hiss has been measured with three-component VLF receivers developed and manufactured at the Polar Geophysical Institute [Pilgaev et al., 2021]. Both receivers are carefully calibrated using a low-frequency waveform generator developed for this purpose [Pilgaev et al., 2018]. The calibra-

tion made it possible to compare the results of observations at spaced points.

Along with VLF observations, we have also used data from the meridional chain of PPN-NAL stations of the Scandinavian magnetometer network IMAGE [http://space.fmi.fi/image], induction magnetometers at LOZ and BAB, all-sky cameras of the Scandinavian observatories Sodankylä (SOD, F=63.92°, Λ=107.26°) and Kevo (KEV, F=66.32°, Λ=109.24°), as well as data from ground-based observations of GPS signals recorded on islands Bear (BJN, F=71.45°, Λ=108.07°), Hopen (HOP, F=73.06°, Λ=115.10°), Longyearbyen (LYR, F=75.12°, Λ=113.00°), and New Aalesund (NAL, F=75.25°, Λ=112.08°) [Oksavik, 2020]. Figure 1 presents a geographical map with ground observation points.

1.1. Analysis of VLF observations

We have preprocessed data from digital recording of VLF-field components by removing pulse signals of atmospherics, caused by lightning discharges, and power-line harmonics. This allowed us to analyze the field at frequencies above 2–4 kHz.

We examined the features of the dynamics of the location of the region on the Earth surface illuminated by auroral hiss bursts (hereinafter the illuminated region) [Nikitenko et al., 2022, 2023], by analyzing emission magnetic field polarization and the direction of wave arrival at the observation point.

To estimate the polarization, we have employed the circular polarization index P_c [Rytov, 1966]. It varies from –1 to +1 [Rytov, 1966]; for waves with right-hand (left-hand) polarization it takes positive (negative) values. In a right-handed polarized wave, the magnetic field vector rotates in the direction of electron rotation in the geomagnetic field [Stix, 1992]. P_c=0 means that waves are linearly polarized, $|P_c|$=1 implies circular wave polarization. To estimate the direction of wave arrival at the observation point, we calculated the azimuthal angle of the vector inverse to the Poynting vector. In this paper, the azimuth angle is measured from the direction to the north.
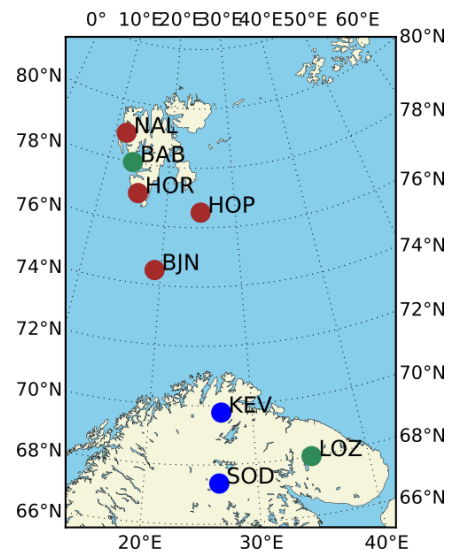

Figure 1. Map of points of auroral hiss observations (green circles), GPS scintillation (red), and auroras (blue) in geographic coordinates

When estimating azimuthal angles, we studied their distribution densities [Nikitenko et al., 2022; Lebed' et al., 2019]. The maximum of the distribution of azimuthal angles shows the most likely direction to the center of the illuminated region [Lebed' et al., 2019]. In order to analyze the temporal dynamics of the location of the illuminated region, we selected short intervals of 1 s to calculate the distribution of azimuthal angles. Transposing the calculated distributions into columns and placing them one after another, we formed time scanning of φ_S. This allowed us to analyze the temporal dynamics of the location of the illuminated region.

2. OBSERVATIONAL RESULTS

Figure 2 exhibits magnetograms of high-latitude IMAGE stations constructed for three 4-hour intervals, including observation intervals of the events under study. Auroral hiss is seen to occur during geomagnetic substorms whose development begins at auroral latitudes (MUO-SOR), after which the region of geomagnetic disturbances moves to the pole.

Figure 3, *a*, *d*, *g* presents spectrograms of the horizontal magnetic field component constructed from observations at LOZ and BAB for the events of interest. These events are seen to be characterized by the fact that at LOZ the intensity of hiss bursts decreases from the beginning of their appearance, whereas at BAB it increases. A similar pattern is observed for all the six events. The observed variations in the hiss magnetic field may indicate movement of its propagation region from auroral to circumpolar latitudes.

2.1. Auroral hiss and geomagnetic pulsations

Auroral hiss bursts were accompanied by Pi2 and Pi1B geomagnetic pulsations. Figure 3 exhibits spectrograms of the geomagnetic field *X* component in the Pi1B range (0.02–1 Hz), obtained from observations at LOZ and BAB (*b*, *e*, *h*), as well as Pi2 pulsations (8–16 MHz) from observations at the IMAGE network (*c*, *f*, *i*). The classification of Pi1B pulsations into a separate type was first proposed in [Heacock, 1967]. They closely correlate with bursts of auroral intensity and riometric absorption (e.g., [Kangas et al., 1979; Bösinger, Yahnin, 1987]), as well as together with Pi2 pulsations they indicate the onset of a substorm. In all the events, geomagnetic pulsations occur first at auroral latitudes (LOZ), and after a while at circumpolar latitudes (BAB). The beginning of a series of auroral hiss bursts at LOZ and the occurrence of pulsations at auroral latitudes coincided in all the events except for March 1, 2019 at 18:00–20:00 UT. In this event, hiss appeared at LOZ 10 min after the onset of pulsations. Note also that the onset of hiss at BAB coincided with the beginning of a substorm at BJN.

2.2. GNSS scintillation

We have analyzed the results of ground-based observations of phase scintillation of GPS signals at the network of stations at the University of Bergen [Oksavik, 2020] (see location of the stations in Figure 1) during the events considered. The observational results are

presented in Figure 4. We took into account only those satellites whose elevation angle was at least 30 . Scintillation is seen to occur at the most equatorial point of this network (BJN) after the onset of the auroral hiss at LOZ. At other points, the time of scintillation onset increases with increasing geomagnetic latitude. As is known [Kintner et al., 2007], scintillation of satellite signals is caused by their propagation through a region with electron density irregularities in the ionosphere. The observed delay in their onset with increasing latitude seems to indicate the shift of region with irregularities to higher latitudes.

Recording of scintillation at high latitudes is caused by GPS signal propagation in the ionosphere through irregularities with scales from hundreds of meters to several kilometers. Ground-based recording of auroral hiss also indicates the existence of electron density irregularities of similar scales in the upper ionosphere [Sonwalkar, Harikumar, 2000], by which waves are scattered into the propagation cone. Since irregularities of similar scales are necessary for the occurrence of scintillation and hiss scattering, the occurrence of hiss first at LOZ and then at BAB and the observed latitudinal dynamics of scintillation indicate the presence of conditions for motion of the illuminated region to the pole.

2.3. Relationship between the position of the scattering region and geomagnetic activity

We have estimated the location of the illuminated region, using auroral hiss observations at LOZ and BAB, in order to explore a possible relationship between the occurrence of these emissions and the shift of the geomagnetic disturbance region and the GPS scintillation source to the pole.

Event on January 5, 2019, 21:00–22:00 UT.

Figure 5, *a–d* presents the results of calculation of P_c and φ_S at LOZ and BAB for the event on January 5, 2019 at 21:00–22:00 UT. At LOZ before 21:20 UT, P_c is close to 1 (see Figure 5, *a*). This means that the recorded waves had right-hand polarization close to circular. After 21:20 UT, P_c did not exceed 0.2, i.e. almost linearly polarized waves prevailed. At BAB, on the contrary, P_c increased with time from almost zero values to 0.5–0.6. Polarization in this case, on the contrary, changed from linear to right-hand circular.

Waves of magnetospheric origin with polarization close to right-hand circular are recorded in the vicinity of the space region where they leave the ionosphere and propagate in the Earth-ionosphere waveguide. The term "propagation region" is often applied to this region (e.g. [Ozaki et al., 2008]). A direct wave dominates here, which has not reflected from the boundaries of the Earth—ionosphere waveguide. Its right-hand circular polarization is due to the fact that the propagating mode in the anisotropic ionosphere is a mode with this very polarization [Stix, 1992]. Linear and left-hand polarized waves are observed at distances where reflection from the waveguide boundaries begins to dominate. This is due to the presence of more favorable conditions for reflecting left-handed polarized waves than for waves with right-hand polarization. Thus, the polarization changes
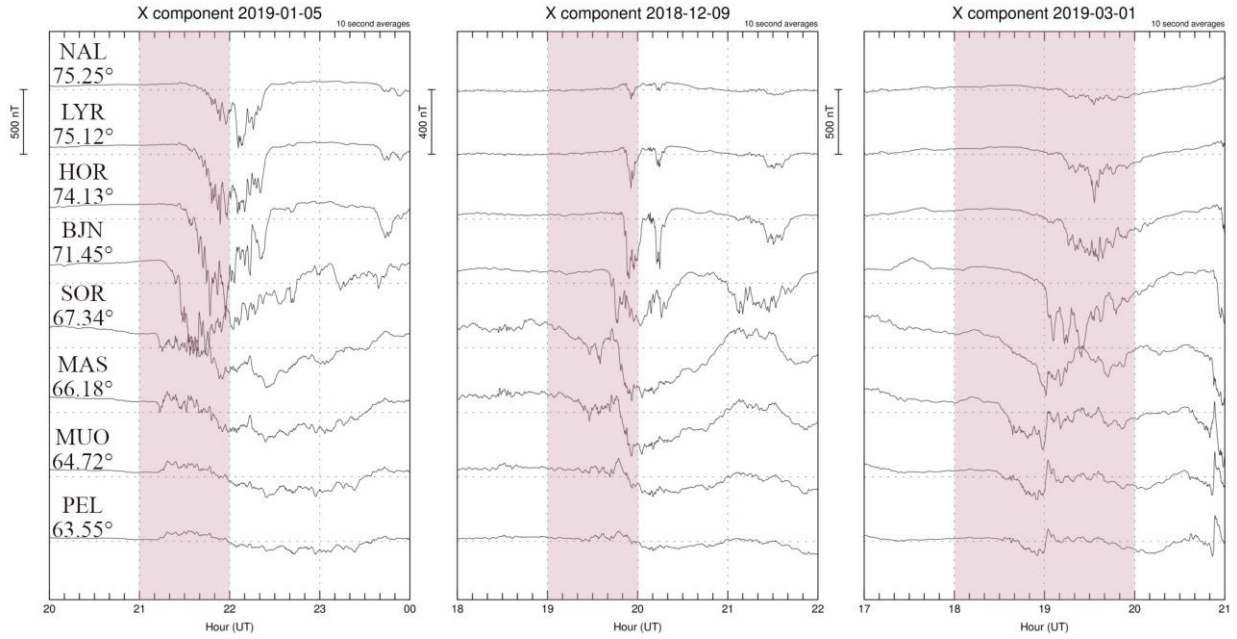
Figure 2. Magnetograms from high-latitude IMAGE stations during the events of interest. The pink field is the time of auroral hiss observation at BAB and LOZ
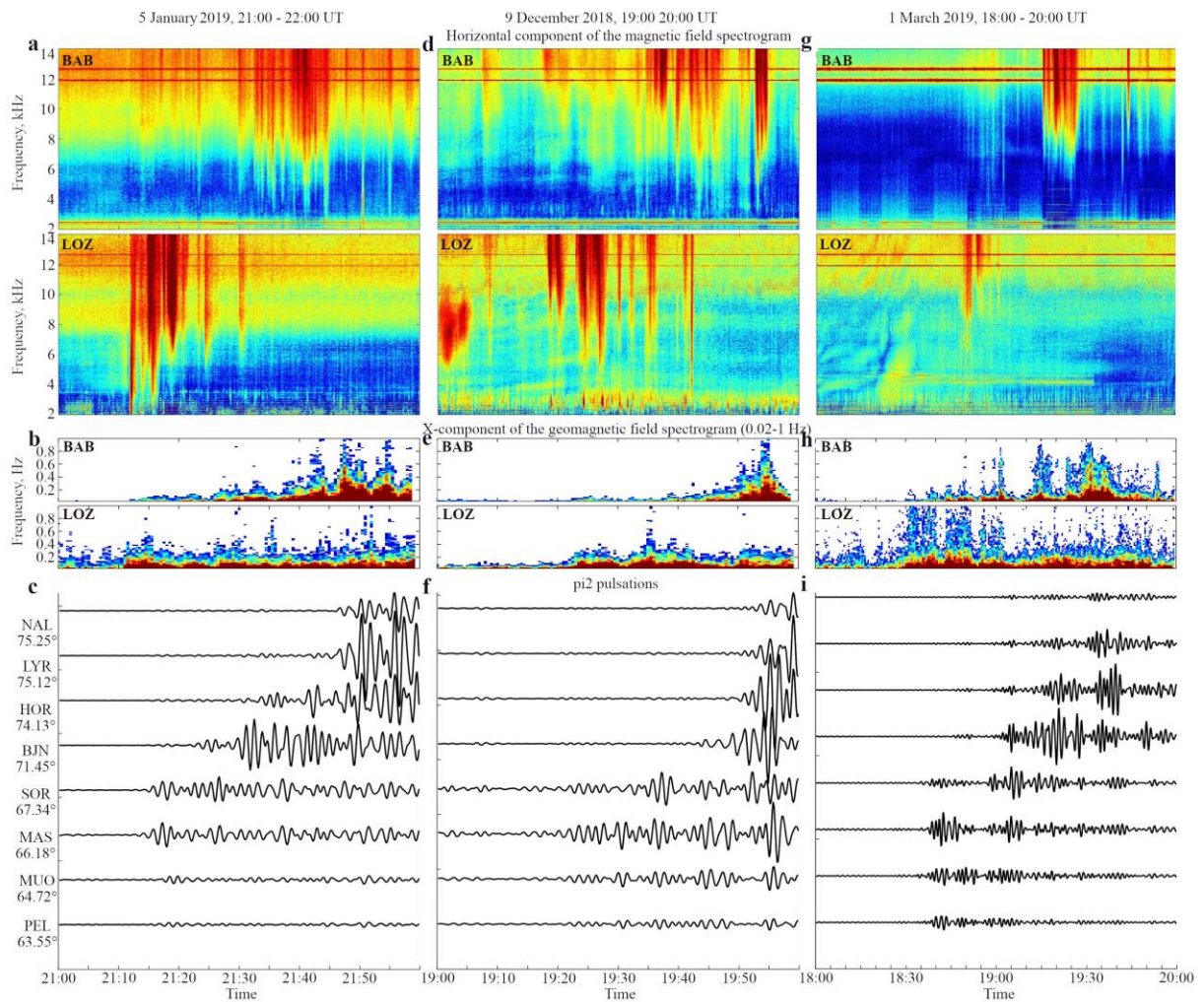

Figure 3. Spectrograms of magnetic field horizontal components in the range 2–14 kHz (*a*, *d*, *g*) and the geomagnetic field *X* component (north-south) in the range 0.02–1 Hz (*b*, *e*, *f*) as observed at LOZ and BAB on January 5, 2019, 21:00–22:00 UT, December 9, 2018, 19:00 UT, and March 1, 2019, 18:00-20:00 UT; Pi2 pulsations constructed from IMAGE magnetometer data during the events under study (*c, f, i*)
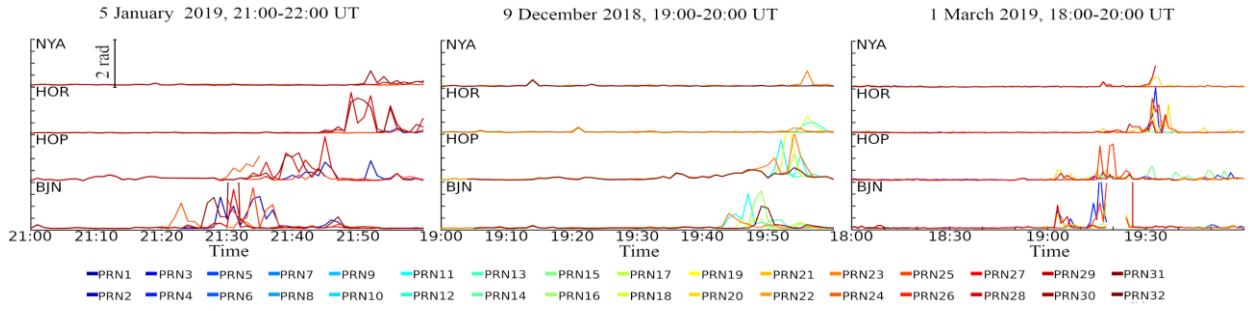
Figure 4. Index of phase scintillation of GPS signals at BJN, HOP, HOR, and NYA on January 5, 2019, 21:00–22:00 UT, December 9, 2018, 19:00–20:00 UT, and March 1, 2019, 18:00–20:00 UT
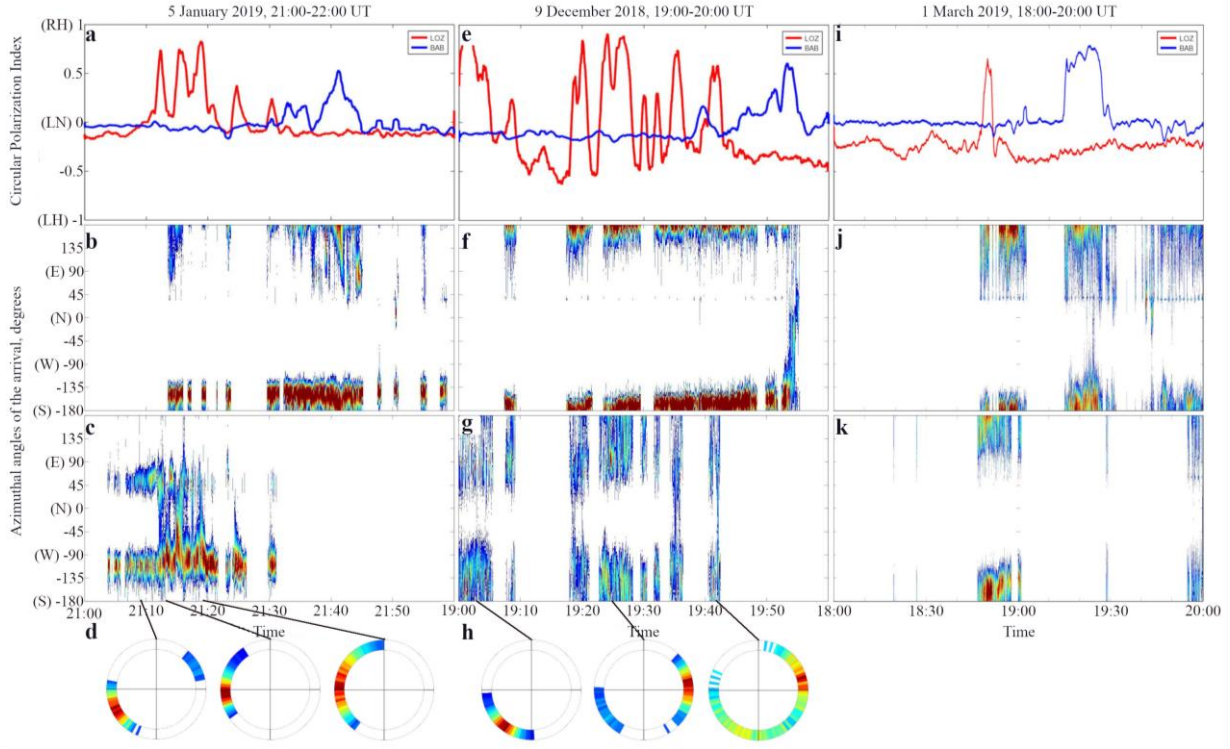

Figure 5. For 21:00–22:00 on January 5, 2019, 19:00–20:00 on December 9, 2018, and 18:00–20:00 UT on March 1, 2019, P_c (*a, e, i*) as observed at LOZ (red) and BAB (blue); sequential histograms of φ_S at BAB (*b, f, j*) and LOZ (*c, g, k*), as well as angle histograms calculated for different intervals from LOZ observations and plotted on a circle (*d, h*)

observed at LOZ indicate the removal of the illuminated region from the observation point. According to BAB data, at that time the illuminated region, on the contrary, approached the observation point.

We analyzed hiss's φ_S to check whether the illuminated region moved to the pole during the events of interest. In Figure 5, *b*, *c* are sequential histograms of φ_S, calculated from LOZ and BAB observations for the event of interest. For clarity, Figure 5, *d* separately shows histograms of angles calculated for three intervals from LOZ observations and plotted on a circle. At LOZ, the position of the maximum of the histograms is seen to vary from –110° at the beginning of observations to –80° at the end. Such variations mean a change in the arrival of waves at the observation point from the west–southwest direction to the west-northwest direction; i.e. the illuminated region moved to higher latitudes in this case. Note that to ~21:16 UT multimode distribution of φ_S was recorded at LOZ at certain points in time. This is likely to imply the simultaneous existence

of several illuminated regions. This situation might have been caused by wave scattering in several zones filled with small-scale irregularities [Nikitenko et al., 2022].

At BAB at the beginning of hiss observation, the φ_S distribution maximum assumed values of ~180° (see Figure 4, *b*). Such angles indicate the direction of wave arrival at the observation point from the south. When maximum hiss intensity and P_c are recorded (see Figure 4, *a*), the maximum of this distribution shifts to ~90°. At that moment, the illuminated region was almost at the same latitude as BAB, but further east of this point. The results also suggest that the illuminated region moved to higher latitudes.

According to the data, hiss bursts occur in the vicinity of LOZ, but their illuminated region moves to higher latitudes. At BAB, on the contrary, hiss is detected with an illuminated region approaching this point. From the results of the analysis, we can assume that the hiss bursts observed at these points can be generated by a single source moving to the pole. Note

that, according to the data, in the vicinity of LOZ the movement occurs along the meridian west of this point, whereas LOZ and BAB are located almost on the same geomagnetic meridian. Unfortunately, the absence of an observation point between them makes it impossible to more accurately trace the path of the illuminated region.

Event on December 9, 2018, 19:00–20:00 UT. The dynamics of P_c and φ_S of the Poynting vector at LOZ and BAB during this event is similar to that observed during the event described above. The measurement results of these parameters are presented in Figure 5, *e*, *h*.

At the onset of hiss bursts at LOZ, P_c was close to 1. When the wave intensity began to decrease (see Figure 2, *d*), its values decreased too. Polarization in this case varied from right-hand circular to elliptical. This, as noted above, is due to the fact that the illuminated region moved away from the observation point.

The maximum distribution of φ_S at the beginning of the series of bursts at LOZ indicates the arrival of waves at the observation point from the southwest, and by the end of this series waves began to arrive mainly from the east-northeast and northeast directions (see Figure 4, *g*, *h*). Thus, the illuminated region passed by LOZ toward higher latitudes in a northeasterly direction.

At BAB, P_c varied from zero, which corresponds to linear polarization, to values close to 1, which are observed at right-hand circular polarization (see Figure 5, *e*). As follows from the observed dynamics of changes in the position of maximum of φ_S distributions, emissions first came to the observation point from the south, and by the end of the bursts the direction of arrival changed to the north and northeast (see Figure 5, *f*).

According to the reasonings given above, during this event the illuminated region moved from auroral latitudes to the pole. Note that despite the general tendency for the illuminated region to shift toward the pole, at auroral latitudes this shift does not occur along the meridian.

Event on March 1, 2019, 18:00–20:00 UT. During this event, unlike the others, there was no uniform motion of the illuminated region in latitude. At the same time, variations in the geomagnetic field, geomagnetic pulsations, and GPS scintillation are similar to those observed in the other five events.

At LOZ, P_c (see Figure 5, *k*) decreases with time, and the wave arrival direction changes from south to southwest after which the bursts abruptly disappear. Thus, the illuminated region approaches LOZ, but does not reach the latitude of the observatory. At BAB, bursts abruptly appear a few minutes after they end at LOZ (see Figure 5, *j*). The P_c index increases slightly with time (see Figure 5, *i*). The position of the maximum of the φ_S distribution remains practically unchanged, which indicates the arrival of waves from the south. In this case, the illuminated region does not reach the latitude of BAB.

To explain the observed jump, we have analyzed data from all-sky aurora cameras and the results of ground-based observations of riometric absorption in

order to investigate the presence of conditions for generating auroral hiss and its propagation to the Earth surface. Unfortunately, due to bad weather it was impossible to analyze auroras at LOZ and BAB; that is why, we used data from KEV and SOD [https://space.fmi.fi/MIRACLE/ASC/asc_keograms_00.shtml] (see the map in Figure 1). Riometric absorption data was taken from the Finnish riometer network [https://www.sgo.fi/Data/Riometer/riometer.php]. Note that for the rest of hiss events discussed above, at auroral observation points on the Kola Peninsula, Fennoscandia, and Svalbard, weather conditions did not allow auroral observations.

Figure 6 presents auroral keograms from KEV and SOD and the results of riometric absorption measurements on March 1, 2019 at 18:00–20:00 UT. It shows that hisses were observed when the auroras moved to the pole. Ground-based recording of hiss is closely related to the occurrence of auroras [Makita, 1979; La Belle, Treumann, 2002], which means that recording of auroras indicates the presence of conditions for hiss propagation to Earth. Movement of the auroras to the pole might have caused the illuminated region to move in the same direction.

The riometer network shows an increase in riometric absorption with increasing latitude. Maximum absorption (~1 dB) was observed to the north of LOZ at IVA and ABI. At this level of absorption, auroral hiss can be observed near the Earth surface [Kleimenova et al., 2019]; however, these riometers usually employ receiving antennas of the wave channel type with apertures of ±45° or wider. Such antennas do not allow us to adequately assess local electron density variations (less than 100–150 km in diameter), which cause attenuation due to the wide antenna pattern [Hunsucker, Hargreaves, 2007]. Therefore, there could be a local region of increased electron density in this event, which could provide a high level of measured riometric absorption in a bounded region and make the ionosphere closed for propagation of the auroral hiss in the vicinity of the observation point.

Since in this event the shift to the auroral pole indicates a shift in the auroral hiss generation region, we assume that
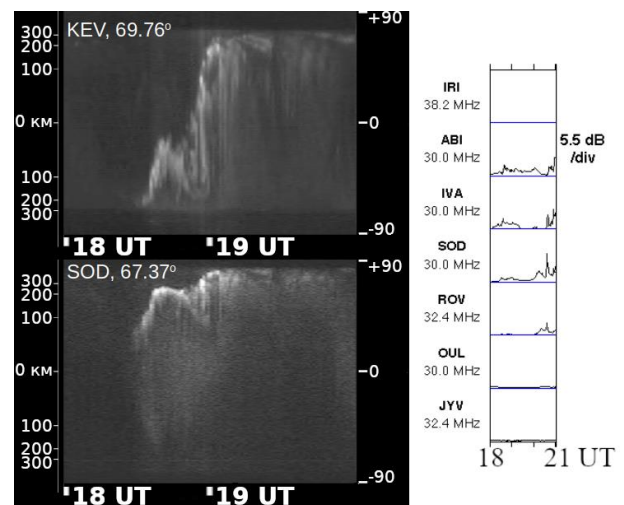
Figure 6. Keograms of auroras from KEV and SOD and results of riometric absorption measurement on March 1, 2019, 18:00–20:00 UT

the abrupt "disappearance" of emission at LOZ might have been caused by the local absence of conditions for its propagation to the Earth surface. The same abrupt changes in the location of the illuminated region, accompanied by an increase in riometric absorption with increasing latitude, were observed in two more of the six cases considered.

3. DISCUSSION

The paper presents the results of the analysis of magnetic field polarization and azimuthal angles of arrival of auroral hiss bursts recorded at LOZ and BAB, and compares these results with data from geomagnetic and GPS scintillation observations. The LOZ and BAB points are located on close geomagnetic meridians in the auroral and circumpolar zones. The events of interest feature a decrease in the intensity of hiss bursts at LOZ from the beginning of their occurrence and their smooth appearance at BAB. The events occur when the geomagnetic disturbance region and the source of phase GPS-signal scintillation move from auroral to circumpolar latitudes.

According to the results of the analysis, the region near the Earth surface illuminated by hiss bursts appears at auroral latitudes and moves to the pole, which is manifested in emission observation first at LOZ and then at BAB. Since the illuminated region, the geomagnetic disturbance region, and the GPS scintillation source move simultaneously and in the same direction, we assume that these processes may be related.

The events in question occur during weak geomagnetic disturbances. The disturbances are accompanied by generation of Pi2 and Pi1B pulsations, suggesting that electrons penetrate into the ionosphere (e.g., [Raspopov, Troitskaya, 1974]). The occurrence of Pi1B-pulsation bursts may indicate the beginning of the development of a local substorm (e.g., [Arnoldy et al., 1998]). The above-described nature of the disturbances and the abrupt shift to the pole after their onset are characteristic of all magnetospheric substorms. The source of the auroral hiss might have been soft electron precipitation typical of substorms.

The VLF auroral hiss propagates to a ground observer due to scattering of waves by irregularities with scales no more than several hundred meters. Irregularities of such scales also determine the observation of GPS-signal scintillation at high latitudes. Observing the simultaneous movement of the scintillation source and the illuminated region suggests that scattering of VLF waves and scintillation of GPS signals occurred by the same irregularities.

A possible cause of the occurrence of electron density irregularities, which ensured propagation of hiss to the Earth surface and caused the occurrence of GPS scintillation, might have been the development of current-convective or (and) drift (type $\vec{E} \times \vec{B}$) instabilities in the ionosphere [Kelley et al., 1982]. The cause for the development of such instabilities is likely to be the amplification of electric fields produced by substorm currents. The presence of such amplification is indicated by the record-

ing of Pi1B geomagnetic pulsations [Wilhelm et al., 1977]. The assumption is confirmed by the results obtained in [Kim et al., 2014]. The authors have found a close temporal and spectral relationship between scintillation and Pi1B geomagnetic pulsations, which allowed them to link geomagnetic disturbances and amplification of electric fields with ground-based recording of GPS scintillation.

The results are consistent with the results of our previous work [Nikitenko et al., 2024], which deals with the events of simultaneous recording of auroral hiss bursts and Pi1B geomagnetic pulsations. The events differed in that the start and end times of the bursts of hisses and pulsations coincided, and were similar in the dynamics of the location of the illuminated region and their accompanying auroras. Based on the data, it has also been suggested that the occurrence of irregularities by which hisses are scattered is also due to the development of current-convective and (or) drift instabilities in the ionosphere. In this paper, the fact of the presence of irregularities is confirmed by observing GPS scintillation during auroral hiss recording.

As indicated in Introduction, a number of studies have observed a close relationship between the occurrence of auroral hiss and amplification of field-aligned currents [Manninen et al., 2020; Spasojevic, 2016]. We assume that the mechanism of this relationship may involve the effect of field-aligned currents on the formation of ionospheric irregularities by which hiss is scattered into the propagation cone.

CONCLUSIONS

We have analyzed magnetic field polarization and azimuthal angles of arrival of auroral hiss bursts recorded at LOZ and BAB and have compared the results with data from geomagnetic observations and on GPS scintillation. We have examined the bursts that occurred first at auroral latitudes at LOZ and a few minutes later at higher latitudes at BAB. Analysis of polarization and azimuthal angles of the Poynting vector has shown that the region on the Earth surface illuminated by hiss bursts was first located near LOZ and then shifted to higher latitudes.

The auroral hiss bursts were recorded at LOZ and BAB during geomagnetic disturbances, which began to develop at auroral latitudes and then, according to the IMAGE network, shifted to higher latitudes. The occurrence of hiss was accompanied by generation of Pi1B geomagnetic pulsations at LOZ and BAB. At the same time, there was a delay in the time of onset of the pulsations, which coincided with the shift of the illuminated region to the pole.

To the north of LOZ, GPS scintillation was observed by a network of high-latitude stations, whose start time increased with increasing magnetic latitude. These observations indicate that the shift of the illuminated region of auroral hiss to the pole was accompanied by the motion of ionospheric irregularities (with scales no more than several hundred meters), which produced the scintillation. Since irregularities of close scales are responsible for hiss propagation to the Earth surface and for the occurrence of GPS scintillation, we assume that the same ionospheric

irregularities might have been responsible for the ground-based recording of hiss and GPS scintillation. Such irregularities could be caused by creation of current-convective and (or) drift instabilities in the ionosphere due to the development of field-aligned currents indicated by simultaneous recording of Pi1B pulsations.

The results demonstrate a close relationship between hiss activity and substorm dynamics. It has been experimentally shown that in the events considered, termination of hiss at auroral latitudes is caused by a shift of the geomagnetic disturbance region to higher latitudes, rather than by changes in the conditions of wave propagation in the ionosphere.

REFERENCES

Arnoldy R.L., Posch J.L., Engebretson M.J., Fukunishi H., Singer H.J. Pi1 magnetic pulsations in space and at high latitudes on the ground. *J. Geophys. Res.* 1998, vol. 103, no. A10, pp. 23581–23591. DOI: 10.1029/98JA01917.

Bösinger T., Yahnin A.G. Pi1B type magnetic pulsations as a high time resolution monitor of substorm development. *Ann. Geophys.* 1987, vol. 5, pp. 231–238.

Gurnett D.A. A satellite study of VLF hiss. *J. Geophys. Res.* 1966, vol. 71, no. 23, pp. 5599–5615. DOI: 10.1029/JZ071i023p05599.

Harang L., Larsen R. Radio wave emissions in the v.l.f.-band observed near the auroral zone–I occurrence of emissions during disturbances. *J. Atmos. Terr. Phys.* 1965, vol. 27, no. 4, pp. 481–497. DOI: 10.1016 /0021-9169(65)90013-9.

Heacock R.R. Two subtypes of type Pi micropulsations. *J. Geophys. Res.* 1967, vol. 72, no. 15, pp. 3905–3917.

Hoffman R.A., Laaspere T. Comparison of very-low-frequency auroral hiss with precipitating low-energy electrons by the use of simultaneous data from two Ogo 4 experiments. *J. Geophys. Res.* 1972, vol. 77, no. 4, pp. 640–650. DOI: 10.1029/ JA077i004p00640.

Hunsucker R.D., Hargreaves J.K. The High-Latitude Ionosphere and Its Effects on Radio Propagation. N.p.: Cambridge University Press, 2007.

Jørgensen T.S. Investigation auroral hiss measured on OGO-2 and Byrd statiion in terms of incoherent Cherenkov radiation. *J. Geophys. Res.* 1968, vol. 73, pp. 1055–1069. DOI: 10.1029/JA073I003P01055.

Kangas J., Pikkarainen T., Golikov Yu., Baransky L., Troitskaya V., Sterlikova V. Burst of irregular magnetic pulsations. *J. Gephys.* 1979, vol. 46, pp. 237–247.

Kelley M.C., Vickrey J.F., Carlson C.W., Torbert R. On the origin and spatial extent of high-latitude F region irregularities. *J. Geophys. Res.* 1982, vol. 87, no. A6. pp. 4469–4475. DOI: 10.1029/JA087i06p04469.

Kim H., Clauer C.R., Deshpande K., Lessard M.R., Weatherwax A.T., Bust G.S., Crowley G., Humphreys T.E. Ionospheric irregularities during a substorm event: Observations of ULF pulsations and GPS scintillations. *J. Atmos. Solar-Terr. Phys.* 2014, vol. 114, pp. 1–8. DOI: 10.1016/j.jastp. 2014.03.006.

Kintner P.M., Ledvina B.M., de Paula E.R. GPS and ionospheric scintillations. *Space Weather.* 2007, vol. 5, S09003. DOI: 10.1029/2006SW000260.

Kleimenova N.G., Manninen J., Gromova L.M., Gromov S.V., Turunen T. Bursts of auroral-hiss VLF emissions on the Earth's surface at *L*~5.5 and geomagnetic disturbances. *Geomagnetism and Aeronomy.* 2019, vol. 59, pp. 272–280. DOI: 10.1134/ S0016793219030083.

Laaspere T., Hoffman R.A. New results on the correlation between low-energy electrons and auroral hiss. *J. Geophys. Res.* 1976, vol. 81, no. 4, pp. 524–530. DOI: 10.1029/JA081i004p00524.

La Belle J., Treumann R. Auroral radio emissions, 1. Hisses, roars, and bursts. *Space Sci. Rev.* 2002, vol. 101, no. 3, pp. 295–440. DOI: 10.1023/A:1020850022070.

Lebed' O.M., Fedorenko Y.V., Manninen J., Kleimenova N.G., Nikitenko A.S. Modeling of the auroral hiss propagation from the source region to the ground. *Geomagnetism and Aeronomy.* 2019, vol. 59, pp. 577–586. DOI: 10.1134/S0016793219050074.

Maggs J.E. Coherent generation of VLF hiss. *J. Geophys. Res.* 1976, vol. 81, pp. 1707–1724. DOI: 10.1029/JA081i010p01707.

Makita K. VLF/LF hiss emissions associated with aurora. *Mem. Nat. Inst. Polar Res.* 1979, Tokyo. Ser. A. No. 16, pp. 1–126.

Manninen J., Kleimenova N., Kozlovsky A., Fedorenko Y., Gromova L., Turunen T. Ground-based auroral hiss recorded in Northern Finland with reference to magnetic substorms. *Geophys. Res. Lett.* 2020, vol. 47, e2019GL086285. DOI: 10.1029/2019GL086285.

Mosier S.R., Gurnett D.A. Observed correlations between auroral and VLF emissions. *J. Geophys. Res.* 1972, vol. 77, no. 7, pp. 1137–1145. DOI: 10.1029/JA077i007p01137.

Nikitenko A.S., Manninen J., Fedorenko Y.V., Kleimenova N.G., Kuznetsova M.V., Larchenko A.V., et al. Spatial structure of the illuminated area of the auroral hiss based on ground-based observations at auroral latitudes. *Geomagnetism and Aeronomy.* 2022, vol. 62, pp. 209–216. DOI: 10.1134/S00 16793222030124.

Nikitenko A.S., Fedorenko Y.V., Manninen J., Lebed O.M., Beketova E.B. Modeling the spatial structure of the auroral hiss and comparing results to observations. *Bull. Russ. Acad. Sci. Phys.* 2023, vol. 87, pp. 112–117. DOI: 10.3103/S106 2873822700265.

Nikitenko A.S., Fedorenko Y.V., Kleimenova N.G. Simultaneous observations of the very low frequency auroral hiss, auroras, and irregular geomagnetic pulsations at the Lovozero Observatory. *Bull. Russ. Acad. Sci. Phys.* 2024, vol. 88, pp. 338–344. DOI: 10.1134/S1062873823705494.

Oksavik Kjellmar. The University of Bergen Global Navigation Satellite System Data Collection. Dataverse NO. 2020. DOI: 10.18710/AJ4S-X394.

Ozaki M., Yagitani S., Nagano I., Hata Y., Yamagishi H., Sato N., Kadokura A. Localization of VLF ionospheric exit point by comparison of multipoint ground-based observation with full-wave analysis. *Polar Sci.* 2008, vol. 2, no. 4, pp. 237–249. DOI: 10.1016/j.polar.2008.09.001.

Pilgaev S.V., Larchenko A.V., Filatov M.V., Fedorenko Y.V. A function generator for calibration of electromagnetic-field recorders. *Instrum Exp Tech.* 2018, vol. 61, pp. 809–814. DOI: 10.1134/S0020441218060106.

Pilgaev S.V., Larchenko A.V., Fedorenko Y.V., Filatov M.V., Nikitenko A.S. A three-component very-low-frequency signal receiver with precision data synchronization with universal time. *Instrum Exp Tech.* 2021, vol. 64, pp. 744–753. DOI: 10.1134/S00 20441221040229.

Raspopov O.M., Troitskaya V.A. The development of a subburst in geomagnetic pulsations. *Collected Papers "High-Latitude Geomagnetic Research".* Leningrad, 1974, pp. 232–247. (In Russian).

Rytov S. Introduction to Statistical Radiophysics. Moscow, Nauka Publ., 1966. (In Russian).

Sazhin S.S., Bullough K., Hayakawa M. Auroral hiss: a review. *Planet. Space Sci.* 1993, vol. 41, pp. 153–166. DOI: 10.1016/0032-0633(93)90045-4.

Sonwalkar V.S., Harikumar J. An explanation of ground observations of auroral hiss: Role of density depletions and meter-scale irregularities. *J. Geophys. Res.: Space Phys.* 2000, vol. 105, no. A8, pp. 18867–18883. DOI: 10.1029/1999JA000302.

Spasojevic M. Statistics of auroral hiss and relationship to auroral boundaries and upward current regions. *J. Geophys. Res.: Space Phys.* 2016, vol. 121, pp. 7547–7560. DOI: 10.1002/ 2016JA022851.

Stix T. Waves in Plasmas. American Inst. of Physics. 1992.

Wilhelm K., Münch J.W., Kremser G. Fluctuations of the auroral zone current system and geomagnetic pulsations. *J. Geophys. Res.* 1977, vol. 82, no. 19, pp. 2705–2716. DOI: 10.1029/ JA082i019p02705.

URL: http://space.fmi.fi/image (accessed April 22, 2024).

URL: https://space.fmi.fi/MIRACLE/ASC/asc_keograms_00.shtml (accessed April 22, 2024).

URL: https://www.sgo.fi/Data/Riometer/riometer.php (accessed April 22, 2024).

How to cite this article
Nikitenko A.S., Kleimenova N.G., Fedorenko Yu.V., Beketova E.B. Ground-based observations of the VLF auroral hiss at Lovozero and Barentsburg observatories. *Solar-Terrestrial Physics*. 2024. Vol. 10. Iss. 4. P. 37–45. DOI: 10.12737/stp-104202405.